9: MODELLING THE THERMAL BEHAVIOUR OF SPACES ENCLOSED BY FABRIC MEMBRANES.

9.1 INTRODUCTION.

In the previous chapter a programme of monitoring was described which was undertaken in order to study the thermal behaviour of a range of spaces enclosed by fabric membranes. This study was carried out for two fundamental reasons:-

- To assess which of the characteristics of spaces enclosed by fabric membranes it would be necessary to model in order to properly simulate their thermal behaviour.
- To provide a comprehensive data set against which the accuracy of a model used to simulate that behaviour might be tested.

Analysis of the monitored data suggested that the thermal conditions within spaces enclosed by fabric membranes could not be considered to be uniform but that strong thermal gradients were seen to exist, particularly during periods of bright sunshine or artificial heating. These gradients resulted from variations in both internal air temperatures and internal radiant temperatures which were motivated by the contrasting thermal behaviour of the fabric membranes compared to other more conventional internal surfaces such as the floor. .

Because of these variations in internal conditions, it was considered that predicting the thermal behaviour of such spaces would require an approach which allowed both radiant and air temperatures to vary from place to place within geometric representations of those spaces.

In this chapter the processes necessary to adopt such an approach are described and the selection of a model appropriate for this purpose is explained. The accuracy of that model is then tested using the monitored data presented in Chapter 8.

9:2. THE MODELLING PROCESS.

9:2.1 The Aims of the Modelling Process.

The spatial modelling process described in this chapter had two fundamental aims:-

- To provide a further insight into forces motivating the thermal behaviour of spaces enclosed by fabric membranes.
- To assess the ability of current theoretical techniques to accurately simulate that behaviour.

In order to satisfy these aims, it was necessary to use a modelling technique which was able to simulate the thermal behaviour of spaces in a way comparable with the monitored data presented in the previous chapter. This behaviour had been monitored based on the CIBSE *resultant temperature* which had been selected as a measure of the thermal conditions that would be felt by the occupants of spaces enclosed by fabric membranes. The resultant temperature (t_{res}) is defined as:-

$$t_{res} = [\, t_r + t_i \sqrt{(10V_i)}\,] \,/\, [\, 1 + \sqrt{(10V_i)}] \qquad [1]$$

In order to simulate the monitored data therefore, it was necessary to predict the *radiant temperature* (t_r), the *air temperature* (t_i) and the *air velocity* (V_i) within the enclosed spaces.

It had been seen from the monitored data presented in Chapter 8 that all of these conditions could vary significantly from place to place within spaces enclosed by fabric membranes and so simulating the monitored data also required an approach which allowed these conditions to vary from place to place.

Theoretical techniques for predicting *radiant temperatures* within an enclosure are complex but relatively well established, based on the geometrical relationships between the surface temperatures enclosing that space. Predicting *air velocities* and *air temperatures* within an enclosure however requires an understanding of the theory of *fluid flow*, and this involves one of the most complex branches of applied mathematics.

9:2.2 The Investigation of Fluid Flow.

The term *fluid* refers to any '*...substance, such as liquid or gas, that can flow...*'[2]. Fluid flow was first investigated experimentally using *physical modelling* techniques such as wind tunnel testing, saline solution analysis and so on. Over the last hundred years however, a second approach developed involving *theoretical analysis* based on the Navier-Stokes equations of pure fluid flow. These equations describe the behaviour of fluid systems at a molecular level and were derived from the laws of conservation of mass, conservation of energy, and Newton's second law[3].

When early attempts were made to simulate fluid flow within large systems such as those found within the built environment, it proved computationally impractical to investigate behaviour at a molecular level. Instead, a more broad approach was adopted which involved predicting the behaviour of a large number of interrelated elements which in combination were representative of the behaviour of the fluid as a whole.

In order to predict the affect of molecular mechanisms such as turbulence and diffusion at this larger scale, it was necessary to develop reduced versions of the pure equations of fluid flow. The process of solving these equations in order to predict the behaviour of large systems now forms the basis of a third branch of fluid flow analysis which is known as *Computational Fluid Dynamics* (CFD)[4].

9:2.3 **Computational Fluid Dynamics.**

CFD techniques were developed in the early 1970's, primarily for use in the aerospace and nuclear power industries. The recent increase in computer speed and information storage capacity however, has meant that CFD models have now become real alternatives to experimental techniques for a wide variety of analytical applications. Such applications range from two dimensional air foil investigations, to complex three dimensional models used for the simulation of sediment deposition.

A list of commonly available CFD codes is maintained by Warsaw University[5], and currently this list includes 72 models, 46 of which are marketed as commercial packages. A number of these models were specifically developed for investigating the thermal behaviour of spaces found within the built environment.

There are several different forms of CFD analysis, however methods such as *finite element* analysis are uncommon within the built environment, where most simulations are based on the assumption of *finite volume*[6].

Finite volume codes define the spatial domain being modelled in terms of a number of dynamically linked volumes whose combined behaviour is representative of fluid flow within the enclosure as a whole. When additional heat transfer mechanisms such as conduction and radiation are added to basic fluid flow models, CFD codes can begin to form truly practical investigative tools. Such tools are particularly appropriate for simulating the thermal behaviour of large and complex spaces for which the traditional assumption that internal conditions are uniform may be inappropriate.

Finite volume codes appropriate for studying fluid flow within the built environment are included in models such as *Flovent*, *Flow-3D*, *Fluent*, *Phoenics* and so on[7]. The mathematical basis of these models is similar, however their format may vary according to the specific use for which they are intended. These differences generally occur at the user interfaces, with a variety of pre and post processing alternatives defining the method of problem specification and controlling the output of results.

For the purposes of this research a model was required which was able to predict internal *resultant temperatures*. This required that it must be able to predict the radiant temperature (including any solar contributions), the air temperature and the air velocity for each finite volume throughout the space being modelled.

With this particular requirement in mind, the general purpose code *Flovent* developed by Flomerics was selected. This package is commercially available, offers good visualisation of both the problem specification and results, and provides a good range of information input alternatives. Flovent is also capable of carrying out detailed comfort calculations throughout the simulated space based on the CIBSE *resultant temperature*. This allowed the model output to be compared directly to the monitored data presented in Chapter 8.

9:2.4 **General Description of *Flovent*.**

Flomerics describe *Flovent* as '*... a practical tool meeting the needs of the designer of heating, ventilating and air-conditioning systems for buildings and similar structures of all types and sizes*.'

Two basic types of simulation can be carried out using Flovent:-

- *Steady state* simulations, in which the domain specification is set constant, and the model solves for a stable solution under those conditions.
- *Transient* simulations, which track the way that internal conditions change through time as a result of a series of thermal events. This second approach is obviously more realistic, however both the problem specification and the computational process are considerably more complex, and the ability to accurately specify the '*start*' conditions can greatly influence the behaviour predicted by the model.

Flomerics recommend that it is usually sufficient to adopt the steady state approach, and that it is most efficient for the user to develop their own thermal boundary model '... *to predict the surface temperatures for a selected instant and then Flovent can provide a steady state solution for that snapshot in time*'[8].

As Flovent has no facility for varying internal surface temperatures with time, it was actually only possible to adopt this steady state approach for the particular purposes of this research. This required that internal surface temperature at a particular instant were generated by the thermal boundary model described in Chapter 7, and this seemed to validate the overall approach adopted for this research.

The basic computational process used by *Flovent* is illustrated by *Figure 9:2.4 below*.

Figure 9:2.4 Schematic Illustration of the Computational Process used by Flovent.

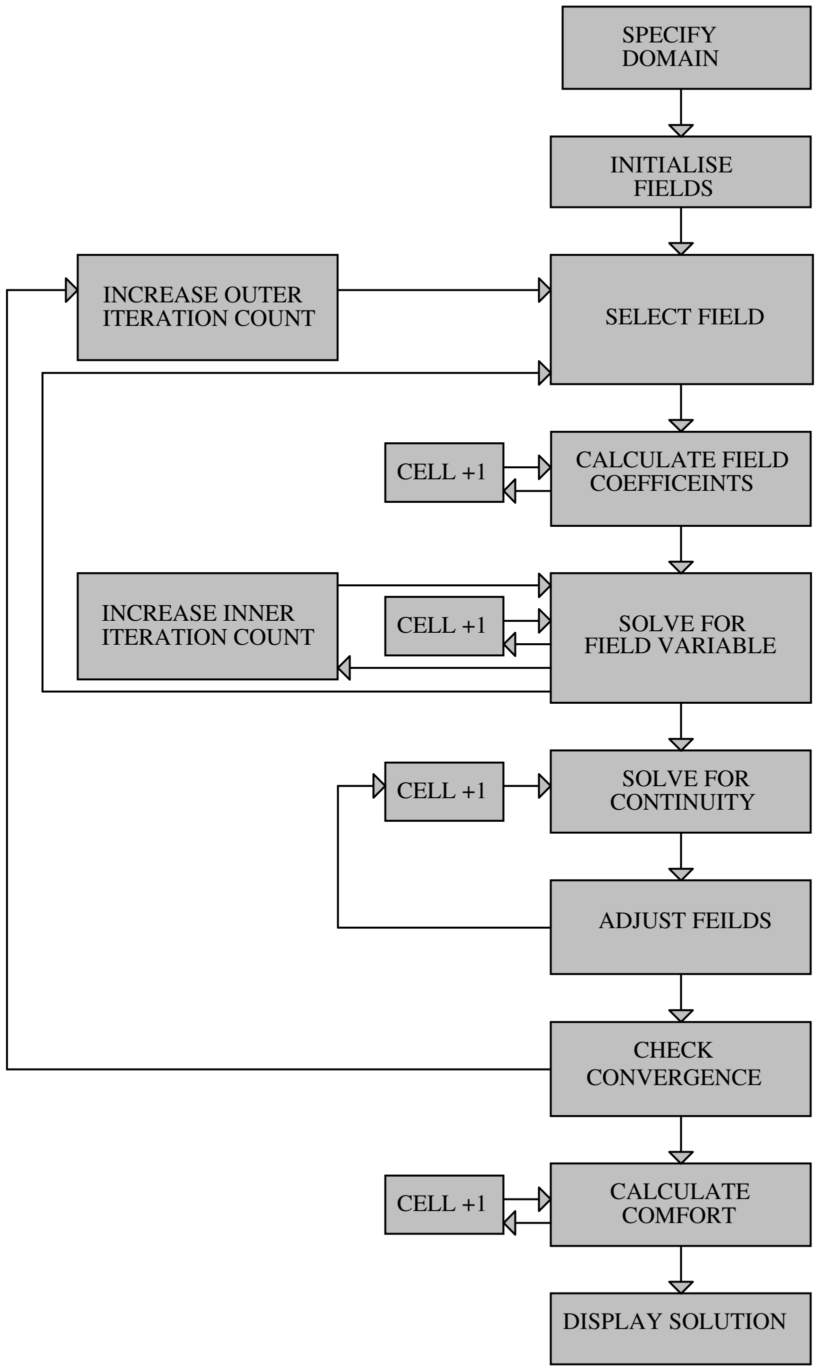

In order to begin a simulation the overall area to be modelled must first be defined by the user, and this is called the '*domain of integration*'. This domain is then divided into a Cartesian grid of finite volume or '*cells*', within each of which thermal conditions are predicted. The finer the mesh of this Cartesian grid, the more precisely the predicted behaviour should represent the reality, however the penalty for this increase in accuracy is a longer computational time and greater data storage requirements.

In order to determine the pattern of air movement and air temperature within each cell, the governing equations of fluid flow are solved for a number of field variables:-

- Velocity in the u direction.
- Velocity in the v direction.
- Velocity in the w direction (if a three dimensional simulation is being carried out).
- Temperature.
- Pressure.

The purpose of these field variables and their deviation is described below:-

- The u, v and w velocities within the each cell describe the air movement in Cartesian directions x, y and z, respectively, and these are solved in order to satisfy the equations for the *conservation of momentum*.
- The cell temperature is solved in order to satisfy the laws of the *conservation of thermal energy*,
- The cell pressure is derived from the equation of continuity which relates to the *conservation of matter*.

NB Two other field variables, Ke turbidity and Diss turbidity may also be calculated if the K epsilon turbidity model is activated, and this is discussed further in the next section.

These field variables are given initial values by the user, and so the job of the model is to adjust the initial values within each cell until a point is reached where the conservation equations are satisfied throughout the domain of integration. This is done by a process of iteration as described below.

Each of the field variables (V) within each of the cells are linked to the similar field variables within each of its six nearest neighbouring cells (V_n, where n = 1 to 6) by the conservation equations. It is also linked to its own field value during the previous iteration (V_0) by inertia. Hence at any stage during the solution, the value of each field variable for each cell is given by the general equation:-

$$V = \frac{C_0V_0 + C_1V_1 + C_2V_2 + C_3V_3 + C_4C_4 + C_5V_5 + C_6V_6 + S}{C_0 + C_1 + C_2 + C_3 + C_4 + C_5 + C_6} \qquad [9]$$

Where coefficients $C_{(n)}$ linked the field values of each of the cells to its neighbours, and S denotes any boundary conditions acting on that cell.

At each outer iteration, the coefficients linking the field variables of each cell to its neighbours (C_n) are calculated and set constant. During each inner iteration these fixed coefficients are then used to solve for the field variables according to the governing equations. This process gives the solution equations the appearance of linearity.

The inner iteration sequence repeats x times for each field variable based on the number of inner iterations specified by the user, then the coefficients are recalculated and another outer iteration begins. When the error of the conservation equations for each of the field variables within each cell reaches zero, it may be considered that the model has converged upon a solution for the fluid flow within the domain.

As the solution process is an iterative one however, it is entirely possible that an exact solution will never be achieved. In practice therefore a termination residual is set by the user, such that when the total error of the conservation equations has fallen below the termination residual, the model is considered to have converged upon a solution. In order to assess the stability of this approximate solution, it is possible to specify monitor points within the domain of integration at which the value of field variables can be tracked between successive iterations. When conditions at these points remain stable from one iteration to the next, then the model can be considered to have converged upon a solution.

Left to itself, *Flovent* can take many thousands of iterations to converge upon a solution, however there are various means by which it can be forced to solve more quickly:-

- An initial value has to be set for each of the field variables, and the more accurate this initial '*guess*', the more quickly the model will converge on a solution.
- The values of each of the field variables can be held within set limits. This can prevent unphysical values such as negative density, and often allows the solution to converge more realistically.
- The number of inner iterations performed to solve the linear equations within each outer iteration can be varied for each of the field variables. This is particularly useful in simulations where behaviour is especially sensitive to variations in one or more of the field variables (typically pressure).
- *Classical linear under relaxation* can be used to as a means of controlling the inertia of the field values between successive inner iterations.
- *False time step under-relaxation* can be used to control the amount by which newly calculated field values are allowed to affect the overall progression of the solution from one outer iteration to the next.
- *Successive over relaxation* can be applied to give inertia to the progression of the linear equations at outer iteration level.

Once the model has solved for the *fluid flow* within the domain, internal resultant temperatures can be calculated. These are based on the *air temperature*, *air velocity* and *radiant temperature* within each cell, where the radiant temperature is calculated from the view each cell has of the surfaces which surround it, and the intensity of solar radiation passing through it.

9:2.5 The Approach Adopted for the Modelling Process.

In the next four sections, the processes undertaken in order to simulate the thermal behaviour of the spaces investigated in Chapter 8 is described, and the accuracy of this process is assessed. The behaviour of the four spaces was simulated using the steady state approach based on those instances from the monitored data presented in Chapter 8 which were considered most characteristic of the observed behaviour.

The problem specification for individual simulations involved two basic processes:-

- Thermal specification of the *boundaries* which enclosed the space to be modelled.
- Thermal specification of the *fluid* contained within that space.

- *Boundary Specification.*

  The purpose of this part of the problem specification was to describe the boundary elements which defined the space to be modelled. These elements could be categorised as either *boundary walls, internal walls, doors, windows, obstructions,* or *HVAC systems* (including *extract fans*, *supply fans*, *internal fans*, *openings*, and *heat sources*).

  The model considered that these elements could affect the thermal behaviour of the space they enclosed as a consequence of four basic parameters:-

- Their geometry
- Their internal surface temperature
- The air which they allowed into or out of the enclosure.
- The quantity of solar radiation which they directed into the enclosure (this was only taken into account when calculating internal radiant or resultant temperatures, *Flovent* did not considered that solar radiation affected fluid flow within the space).

- The *geometry* of the enclosures was interpreted from construction information obtained from the building owners. Flovent however was a finite volume CFD code, for which the domain specification was based upon a Cartesian grid. This meant that the characteristic curvature of the membrane envelopes had to be represented by a series of horizontal and vertical panels enclosing a grid of finite volume cells. Obviously, the smaller the grid mesh size, the more accurately these boundary panels represented the actual curve of the fabric but the greater the computational overhead. The grid spacing could be made to vary throughout the domain of integration in order to accommodate boundary elements of different size and significance.

- The *internal surface temperatures* of the horizontal and vertical panels of the fabric membrane boundaries were determined using the thermal boundary model described in Chapter 7. In order to specify the boundary model, the properties of those membranes which it had not been possible to determine experimentally had to be estimated. This was done based on the properties of similar membranes and any available manufacturers information. This, and the experimental information presented in Chapter 6 produced the data set of material properties presented below.

Figure 9:2.5 Table to Summarise the Properties Used to Predict the Thermal State of the Fabric Membrane Boundaries.

	Landrell Factory	Eisteddfod Arena	Administration and Amenities Building	AELTC Covered Courts
near normal translucency	3.7	10.0	16.2	9.8
near normal absorptance	50	14.7	14	35.5
near normal reflectance	46.3	75.3	69.8	54.7
diffuse solar translucency	2.9	7.8	12.6	7.3
diffuse solar absorptance	48.8	15	15.5	31.5
diffuse solar reflectance	48.3	78.4	73	61.2
int surface near normal emissivity	0.92	0.91	0.92	0.92
ext surface near normal emissivity	0.92	0.91	0.92	0.91
near normal long wave translucency	0.03	0.03	0.02	0.03
core conductivity	320	320	320	270

The temperatures of other internal boundaries were determined from the monitored data presented in Chapter 8.

- The quantity of *air* which the HVAC boundaries allowed into or out of the enclosure was determined either from the monitored data, based on wind speeds or surface pressures, or from manufacturers specifications of mechanical ventilation systems.

- The quantity of *solar radiation* which the membrane panels directed into the enclosure was determined using the solar model described in Chapter 7. This model assumed that solar radiation transmitted into the space was totally diffuse however *Flovent* only allowed direct beam solar radiation to be specified. This meant that diffuse internal conditions had to be achieved by specifying a uniform transmittance for the whole membrane boundary, and then positioning the sun directly overhead.

The intensity of this uniform transmittance was determined by calculating the actual quantity of solar radiation directed into the enclosure by each membrane panel ($A \times q_{\tau}$), and then predicting the average transmittance of the entire membrane (τ_{av}) from these values.

$$\tau_{\mathrm{av}} = H \,/ \left[\frac{\sum_{i=1}^{n} \left(\mathrm{A_n} \times \mathrm{q}_{\tau} \right)}{A} \right]$$

where H is the intensity of horizontal global solar radiation, A_n is the area of the individual actual inclined membrane panels (*n)*, and A is the total area of horizontal panels specified.

- *Fluid Properties.*

The physical properties of the fluid which occupied the space being modelled had to be defined in order that its behaviour could be predicted. This involved specifying the fluids *density, conductivity, specific heat, expansivity, viscosity* and *diffusivity*.

For the purposes of this research, the fluid contained by the enclosure was '*air*'. The range of conditions encountered during the monitoring process were fairly specific, and so many of the properties of the enclosed air could be considered to be constant[10]. This meant that the default specifications within Flovent could be used to describe the *density*, *conductivity*, *specific heat*, and *expansivity* of the fluid.

The specification of *viscosity* and *diffusivity* however, could profoundly affect the behaviour of the fluid at a molecular level and so these were more complicated to determine. Flovent provided three alternative methods for ensuring that the correct governing equations of fluid flow were selected in order to represent the molecular behaviour of the enclosed air:-

- It could be assumed that air flow throughout the enclosure was entirely *laminar*. This would have been appropriate if the air consisted of independent '*layers*' which slipped smoothly over one another with little molecular interaction.

- If internal conditions were such that significant disturbance of laminar flow was likely to occur throughout the space, then air movement could be considered to be entirely *turbulent*. In this case, the turbulent viscosity of the air had to be specified by the user, and this could be determined using the simple calculation overleaf.

turbulent viscosity = 0.01× characteristic air velocity × characteristic cell length [11]

- In many cases the solution proved insensitive to small variations in the value of turbulent viscosity input by the user. If however, initial tests suggested that a particular simulation was highly dependent upon turbulent viscosity, then the '*k epsilon*' model of turbulence could be activated. This allowed the model to calculate the actual turbulent viscosity within each cell, based on the kinetic energy of turbulence '*k*' and its rate of dissipation '*epsilon*'[12].

It was considered that it would have been incorrect to make assumptions about the behaviour of a space whose behaviour the model was attempting to predict, and so the *k epsilon* model of turbulent viscosity was activated for all the simulations carried out.

The first of these simulations is described below.

9:3. MODELLING THE THERMAL BEHAVIOUR OF LANDRELL FABRIC ENGINEERING.

9:3.1 Specification of Landrell Fabric Engineering.

It was recognised that the Landrell Fabric Engineering building was not entirely appropriate for this sort of modelling. The obscure membrane combination, and in particular the internal liner was difficult to simulate, and modelling the multi peaked doubly curved envelope as a series of horizontal and vertical panels was very laborious. However, similar to the monitoring of this building, the complexity of the problem provided a useful means of testing the range of modelling techniques available.

A simple two dimensional geometry was specified, which was based upon a representative vertical section through the space (see *Figure 8:3.1a*). It was considered that the space was complex enough even in this simple form, without attempting to define its geometry in three dimensions.

The external membrane was specified as a series of *window panels* whose internal surface temperatures and translucencies were determined using the boundary model described in

Chapter 7. The internal liner was treated as a series of fixed *radiant panels* whose temperature was determined from the monitored data presented in Chapter 8. The other internal surfaces were then specified as a series of *boundary walls* whose internal surface temperature was determined from the monitored data presented in Chapter 8.

The factory space was linked to the roof cavity through an apex opening in the internal liner, and the roof cavity was linked to the outside air by free openings in the corner peaks of the external membrane.

Initially only one of the repetitive factory units was modelled, however this resulted in difficulties in accurately specifying the temperature of the air moving between the adjacent factory units. As a consequence of this the factory was re specified as two units, joined together. This produced a domain of almost 4000 cells, 114 cells long and 35 cell high, as illustrated by *Figure 9:3.1a* below.

fig 9:3.1a Model Representation of Landrell Fabric Engineering.

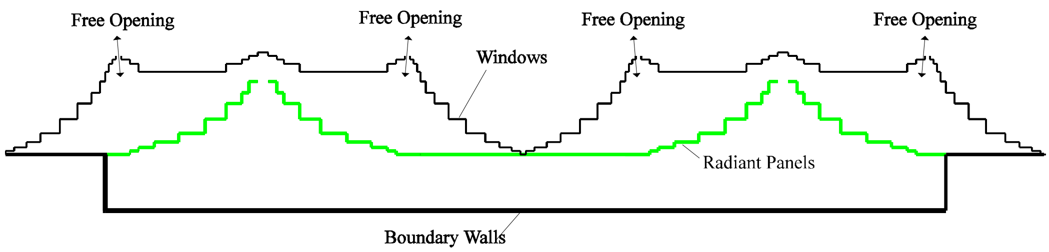

Two simulations were carried out, both based on the data monitored during 1/10/94, the unheated day illustrated in Chapter 8. The first was based on data recorded when conditions within the space had been almost entirely diffuse (0:100), and the other based on data recorded when extreme positive stratification had been monitored within the space (13:30).

The output from these two simulations is presented in *Figure 9:3.2b and 9:3.2c*, overleaf. These diagrams illustrate the internal resultant temperatures and the internal air velocities predicted by *Flovent*. The internal air velocities on both diagrams are illustrated according to the same scale, but two different scales were used for the internal resultant temperatures, one suitable for diffuse conditions, and the other suitable for representing strong internal stratification. These two basic temperature scales are used for all of the *Flovent* output presented in this chapter.

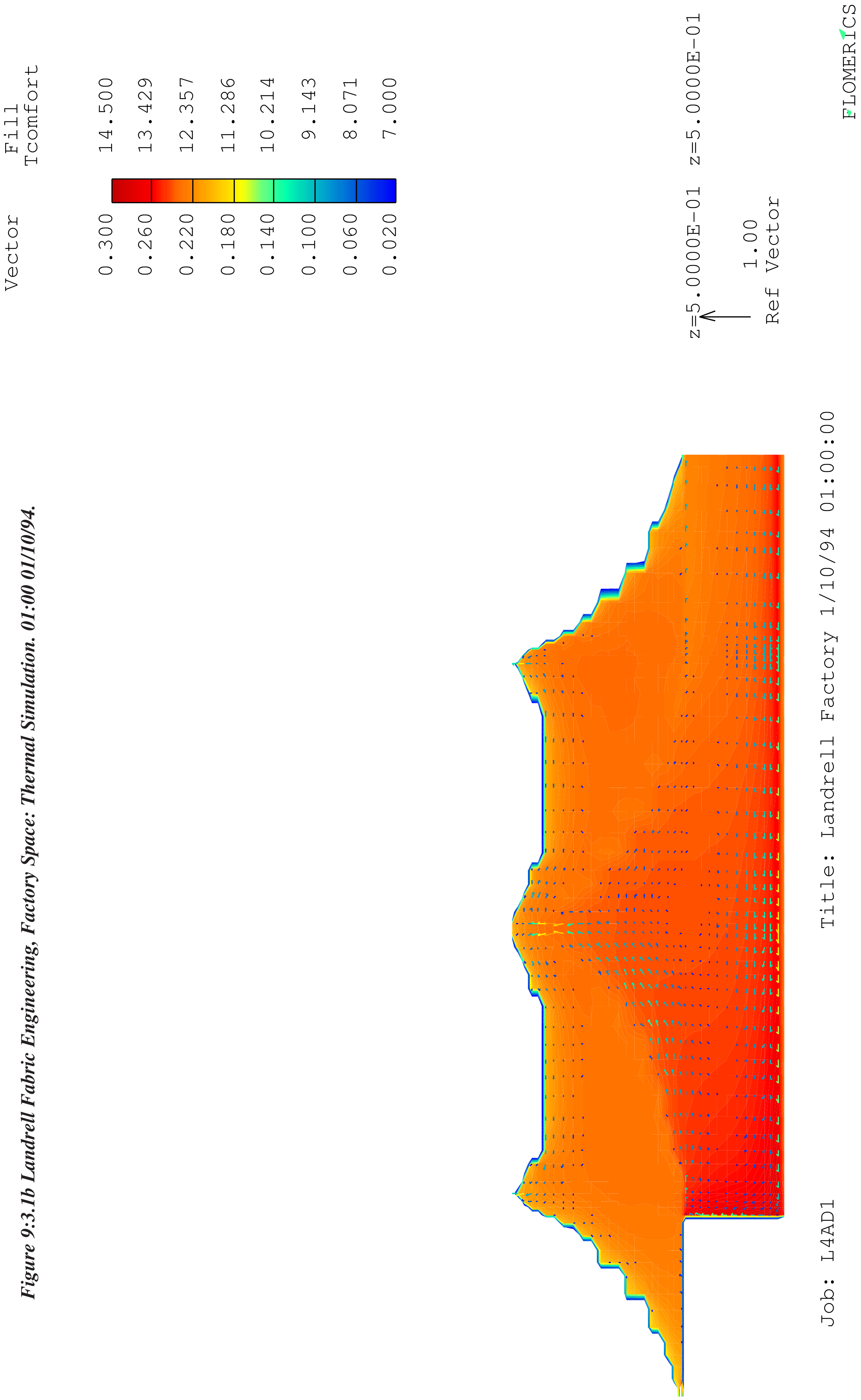

Figure 9.3.1b Landrell Fabric Engineering, Factory Space: Thermal Simulation. 01:00 01/10/94.

Figure 9:3.1c Landrell Fabric Engineering, Factory Space: Thermal Simulation. 13:30 01/10/94.

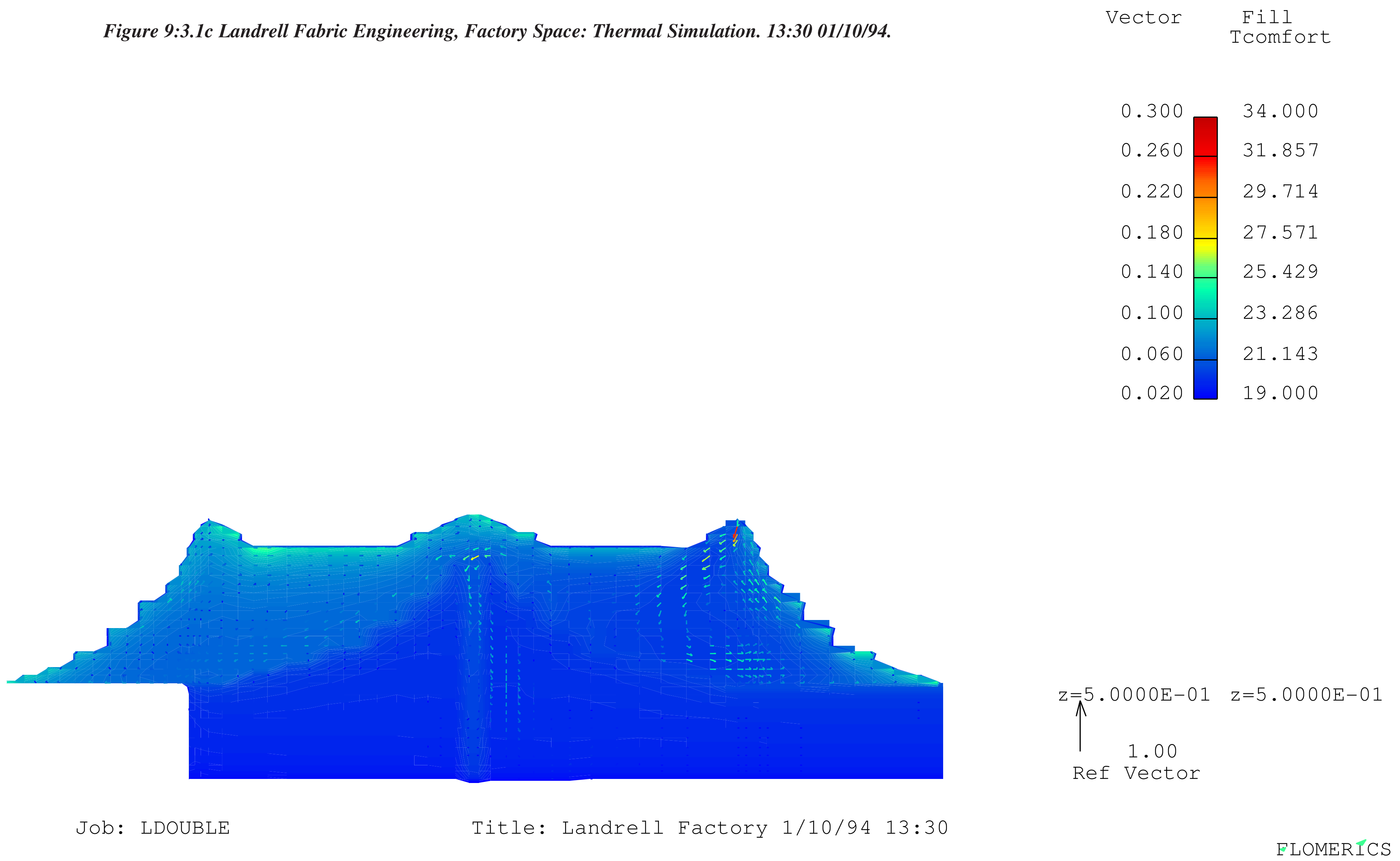

9:3.2 Comparison Between the CFD Model Output and the Data Monitored at Landrell Fabric Engineering.

The relationship between the simulated behaviour shown in *Figures 9:3.1b* and *c*, and the monitored data presented in Chapter 8 is illustrated by *Figure 9:3.2* below. The markers represent the relationship between the resultant temperatures monitored by the eleven sensors within the building, and the temperatures predicted at those locations by *Flovent*. The diagonal line represents the ideal relationship indicative of where the markers would be if there was no difference between the predicted and monitored values.

Figure 9:3.2 Graph to Illustrate the Relationship Between the Monitored and Predicted Resultant Temperatures Within Landrell Fabric Engineering.

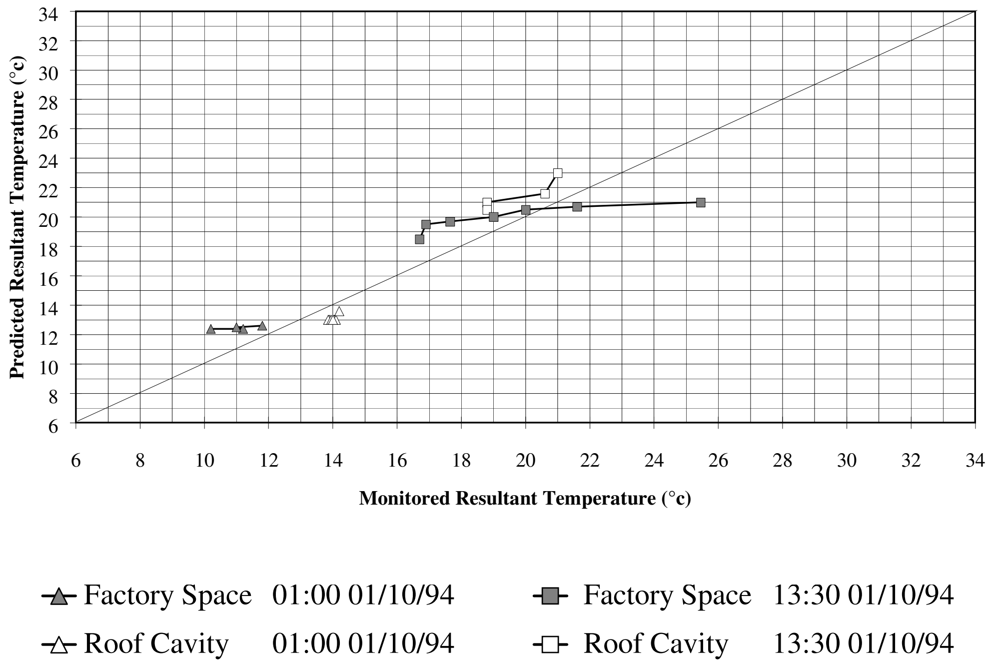

It can be seen that in general, the predicted resultant temperatures followed the same trend as the monitored values, and the spread of makers about either side of the ideal was fairly even.

The behaviour predicted by the first simulation (*Figure 9:3.1b*) was similar to that which had been monitored, i.e. temperatures within the roof cavity were close to the external air temperature, and the factory space itself was slightly hotter. As a result, the average difference between the monitored and predicted resultant temperatures was just 1.1^{o}c. The predicted behaviour did display less of a range of temperatures than had been monitored, but because the internal conditions were relatively uniform at that instant, all the predicted resultant temperatures were within 2.2^{o}c of the monitored data.

The errors apparent from the second time step simulated (*Figure 9:3.1c*) were more significant. Whilst the average predicted internal resultant temperature was within 1^{o}c of the monitored value, the model predicted less of a range of temperature than had been monitored, particularly in the main factory space. Stratification of almost 9^{o}c had been monitored within this space, but *Flovent* had only predicted stratification of 4.5^{o}c and this resulted in model errors of up to 4.5^{o}c. The predicted stratification of internal resultant temperatures was composed of a radiant gradient of over 6^{o}c but internal air stratification of just 2^{o}c, suggesting that the error was caused primarily by the fluid flow model.

These difficulties appeared to result from the compartmentalisation of the space. Predicted air movement patterns within the roof cavity were quite different from those within the main factory space during both instants simulated (see *Figures 9:3.1b* and *c*), and *Flovent* appeared to have difficulty rationalising these differences at the opening in the internal liner where the two spaces met. As a consequence of this the convergence procedure was very slow, and solutions tended to be unstable.

It was difficult to draw any general conclusions from these problems as the simulation of this building posed such an unusual problem. It was obvious however that in order to properly simulate such a complex space, a considerably more detailed specification and so considerably more computational power would be required. Because of the doubly curved nature of the twin skin membrane envelope, this would be a difficult and time consuming procedure, as will be discussed in the final section of this chapter.

It was considered that the simulation of the single membrane Eisteddfod Arena described in the next section would pose a simpler problem, and so the stability of the model solution would be more convincing.

9:4. MODELLING THE THERMAL BEHAVIOUR OF THE EISTEDDFOD ARENA.

9:4.1 Specification of the Eisteddfod Arena.

Because of the depth of the main section (*Figures 8:4.1a and 8:4.1b*), and the relative simplicity of Eisteddfod Arena, it was considered adequate to represent its shape in two dimensions, despite its overall doubly curved geometry. As the external data from the first monitoring session had been incomplete, only data from the second period could be simulated. This data had been monitored during a period when the perimeter extensions had been added to the main arena in preparation for the Eisteddfod.

The extended membrane was defined as a series of 79 horizontal and vertical *window panels* with fixed internal surface temperatures determined using the thermal boundary model described in Chapter 7. The other surfaces which enclosed the space, were specified as *boundary walls*, the internal surface temperatures of which were determined from the monitored data.

This produced a domain of integration which consisted of 4850 individual cells, 88 cells long and 55 cells high, as illustrated by *Figure 9:4.1a* below.

Figure 9:4.1a Royal International Eisteddfod Pavilion, Main Arena: Model Representation.

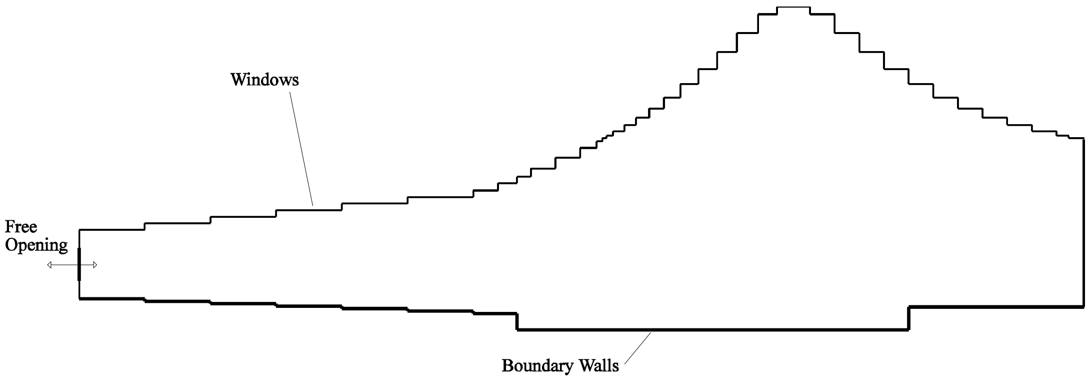

Because the perimeter extensions were added, the space was more tightly sealed than during the winter and so it was considered that the there would only be slight infiltration. For this purpose a small, free opening was specified at the far end of the membrane extensions through which external air was able to penetrate into the enclosure.

Figure 9:4.1b and 9:4.1c overleaf illustrate the internal resultant temperatures and internal air velocities predicted by two simulations which were carried out based on the monitored data previously presented in Chapter 8. Two instants were chosen which it was considered best illustrated the characteristic behaviour of the space. The first was based on data recorded when conditions within the space had been almost entirely diffuse (21:43 24/8/94), and the second was based on data recorded during a period of extreme positive stratification (13:39 25/8/94).

NB After poor initial results were obtained for the second period simulated, the diffuse overhead solar radiation was replaced with angular direct beam solar radiation as indicated on *Figure 9:4.1c*, and the reasons for this will be discussed in the next part of this section. A number of cells on this figure display unusual resultant temperatures which could not be explained by the problem specification. As the air temperatures at these locations appeared realistic however, it was considered that these anomalies resulted from a problem within the solar model which would not effect the accuracy of the solution as a whole.

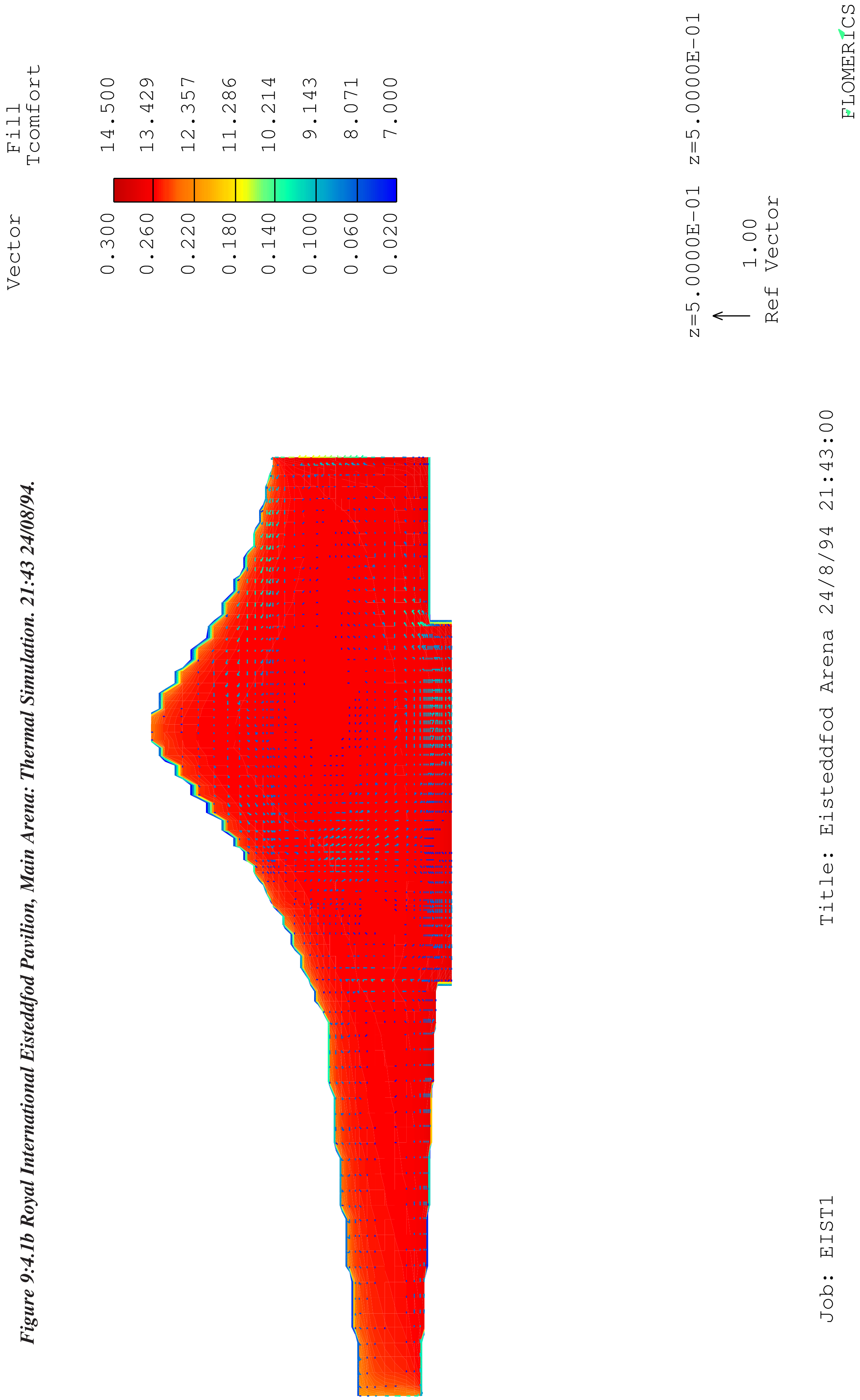

Figure 9:4.1b Royal International Eisteddfod Pavilion, Main Arena: Thermal Simulation. 21:43 24/08/94.

Figure 9:4.1c Royal International Eisteddfod Pavilion, Main Arena: Thermal Simulation. 13:39 25/08/94.

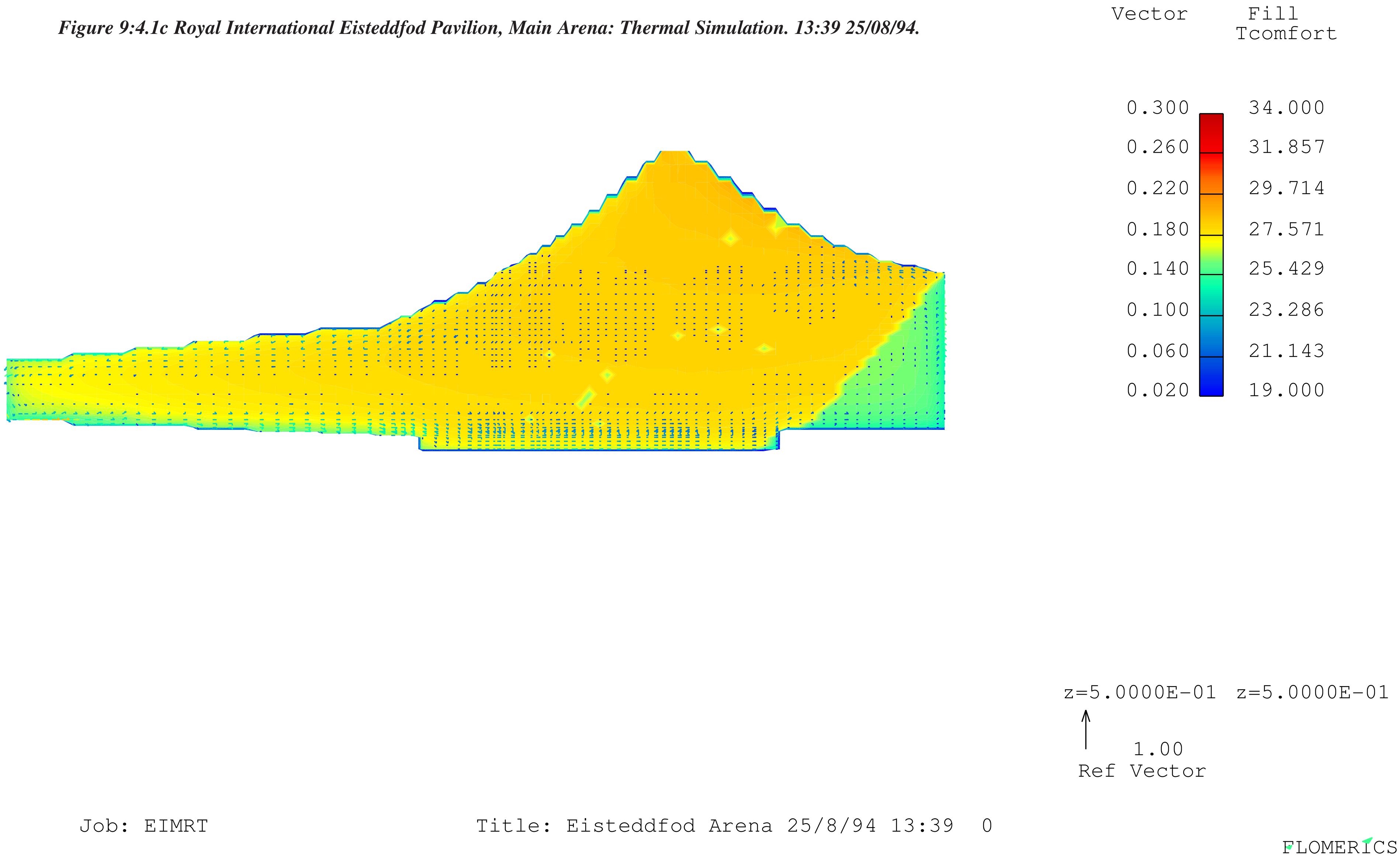

9:4.2 Comparison Between the CFD Model Output and the Data Monitored at the Eisteddfod Arena.

The relationship between the simulated behaviour shown in *Figures 9:4.1b* and *9:4.1c*, and the monitored data presented in Chapter 8 is illustrated below. The markers represent the relationship between the resultant temperatures monitored by the eleven sensors within the building, and the temperatures predicted at those locations by *Flovent.* The diagonal line represents the ideal relationship.

Figure 9:4.2a Graph to Illustrate the Relationship Between the Monitored and Predicted Resultant Temperatures Within the Eisteddfod Arena.

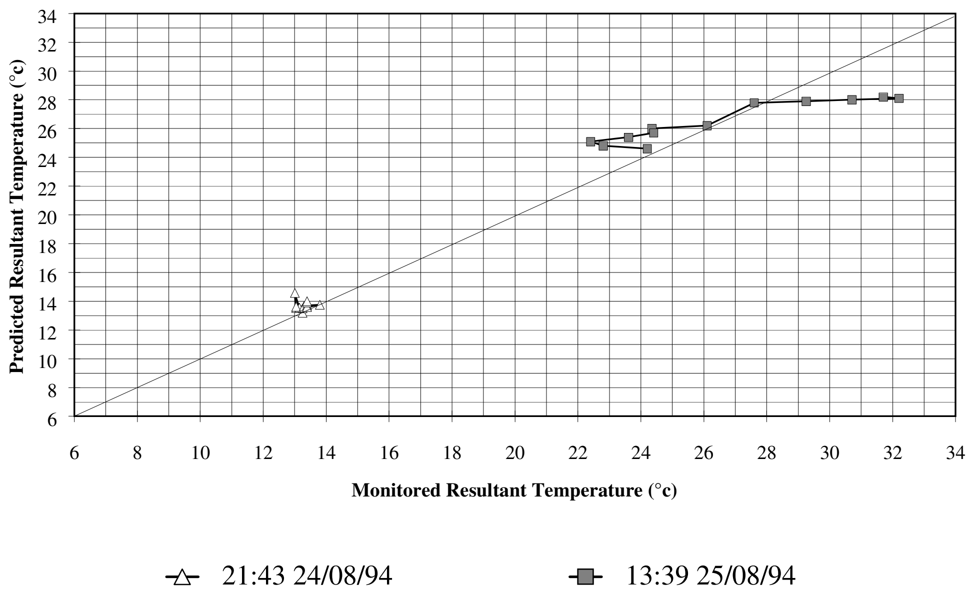

The first simulation presented (*Figure 9:4.1b* 13:39 25/8/94) was considered very accurate. Internal temperatures were all very close to the specified external air temperature, and little internal stratification was predicted. As a result of this, the average predicted internal resultant temperature was within 0.4^{o}c of the monitored value and the maximum model error was just 0.6^{o}c.

As with the Landrell Factory however, simulation became considerably more complex for the second instant, when strong internal thermal gradients were observed. An early attempt to simulate this behaviour which is not presented here produced very poor results, with the model errors of over 6^{o}c. It was considered that this resulted in part from the position of the sun in the sky, which was behind the high south wall at the stage end of the space. If any of the solar radiation penetrating through the membrane were direct beam rather than diffuse, this would place the low level temperature sensors in the shade and increase in the intensity of solar radiation incident upon the high level sensors.

For this reason a second simulation was carried out with the actual solar position specified as indicated by *Figure 9:4.1c.* This produced an average error of just 1.8^{o}c when compared to the monitored data and reduced the maximum model error to 4^{o}c. This suggested that the high transmittance Eisteddfod membrane was only partially diffusing, and this considerably complicated the optical properties information which would be necessary to accurately predict its behaviour. This issue will be discussed further throughout the rest of this chapter.

Even when it was accepted that the Eisteddfod Arena membrane transmitted *only* direct beam solar radiation however, the model still under predicted the range of temperatures found within the space during the second instant. Low level temperatures should have been close to the external air temperature, but were actually significantly hotter, whilst predicted high level temperatures were up to 4^{o}c cooler than the monitored values. As a consequence of this, *Flovent* predicted internal stratification of just 3.3^{o}c, compared to the stratification of 9.8^{o}c which had been monitored,

This predicted stratification of internal resultant temperatures comprised a radiant gradient of over 5^{o}c but internal air stratification of just 0.5^{o}c, and so as with the second Landrell simulation, it appeared that the modelling inaccuracy was caused primarily by a problem within the fluid flow model itself. This is shown clearly by the graph below.

Figure 9:4.2b Diagram to Illustrate the Radiant and Air Temperature Components of the Resultant Stratification Predicted by Flovent (13:39 25/08/94).

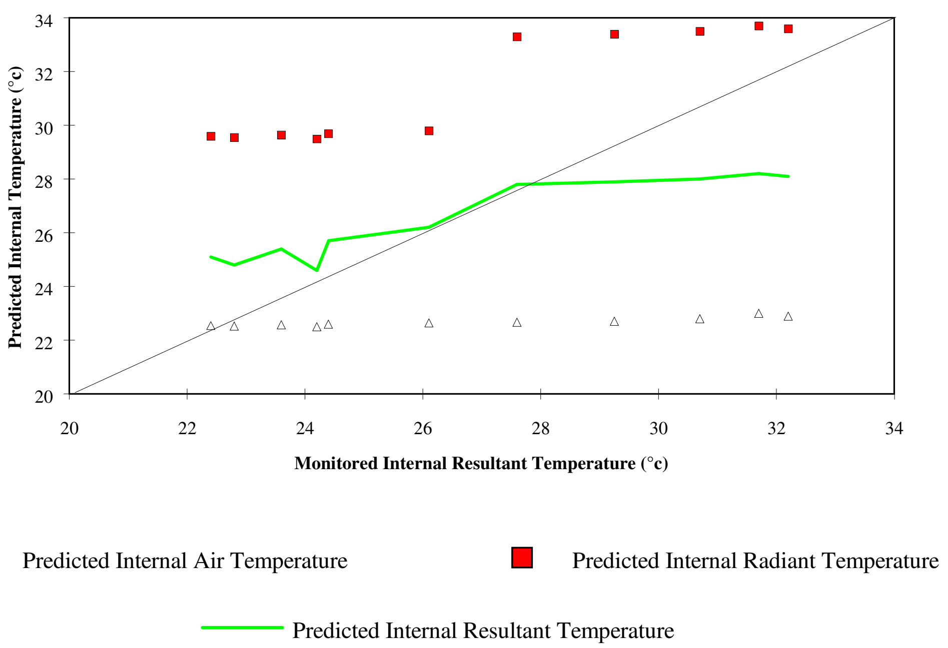

It was considered that the model tendency to underestimate the stratification of internal air in this instance could be caused either by the incorrect specification of *internal surface temperatures*, or an incorrect prediction of *internal air movement patterns*:-

- The validation of the boundary model presented in Chapter 7 suggested that if anything, the temperature of the membrane would be overestimated, and it seemed unlikely therefore that the specification of surface temperatures would result in the underestimation of internal stratification. As high level membrane surface temperatures of over 32^{o}c had been specified, it was also surprising that the maximum internal air temperature predicted at any of the monitor points was just 23^{o}c.

- This suggested that the problem was caused by the internal air movement predictions, either resulting in an underestimation of surface heat transfers, or an over diffusion of internal air temperatures. These two points will be discussed further throughout the rest of this chapter.

9:5. MODELLING THE THERMAL BEHAVIOUR OF THE ADMINISTRATION AND AMENITY BUILDING.

9:5.1 Specification of the Administration and Amenity Building.

It was considered that it would only be possible to accurately represent the thermal behaviour of the space under the distended cone shape of the Administration and Amenity Building roof by carrying out a three dimensional simulation. In order to achieve even a rough approximation of its shape however, this meant that the membrane had to be described in terms of 230 horizontal and vertical *window panels* each of which had to be individually specified and its thermal state determined. This produced an overall domain containing almost 7,500 cells.

The internal surface temperature of the membrane panels was predicted using the thermal boundary model described in Chapter 7. The other surfaces enclosing the space were specified as *boundary walls* and their temperatures were determined from the monitored data. Low level *free openings* were placed around the perimeter of the space to allow the infiltration of air from adjacent spaces into the central atrium (see *Figures 8:5.1a* and *8:5.1b*). High level *free openings* were also specified in order to allow wind to penetrate into the space if required. This allowed the unusual conditions recorded during the first monitored period to be properly investigated.

Figure 9:5.1a The Administration and Amenity Building: Model Representation.

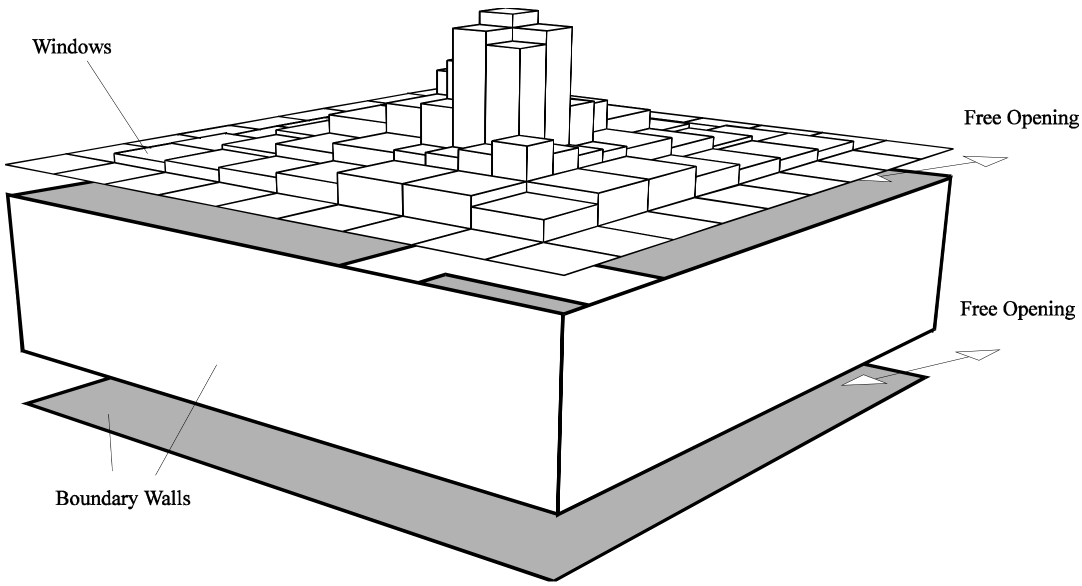

Figure 9:5.1b and 9:5.1c overleaf illustrate the internal resultant temperatures and internal air velocities predicted by two simulations which were carried out based on the monitored data previously presented in Chapter 8. The first was based on the unusual data recorded during the first monitored period when conditions within the space had been almost entirely diffuse (14:00 17/4/94). The second simulation was based on data recorded during the second monitored period when extreme positive stratification had been observed within the space (10:30 11/6/94).

In order to investigate the unusual behaviour observed during the first monitored period, (previously discussed in Chapter 8) the simulation presented in *Figure 9:5.1b* was carried out with a wind of 1.5m/s penetrating into the space from the south west through the high level perimeter louvres. Because of this, the air velocity scale adopted for this diagram is different from that used for the other simulations presented in this chapter.

The sun was oriented directly overhead for both simulations in order to produce uniform solar intensities inside the space. This was considered reasonable as the orientation of the sun during both of these instances was such that none of the internal sensors would have been in the shade even if the transmitted solar radiation had been entirely direct beam.

Figure 9:5.1b The Aministration and Amenity Building: Thermal Simulation. 14:00 17/04/94.

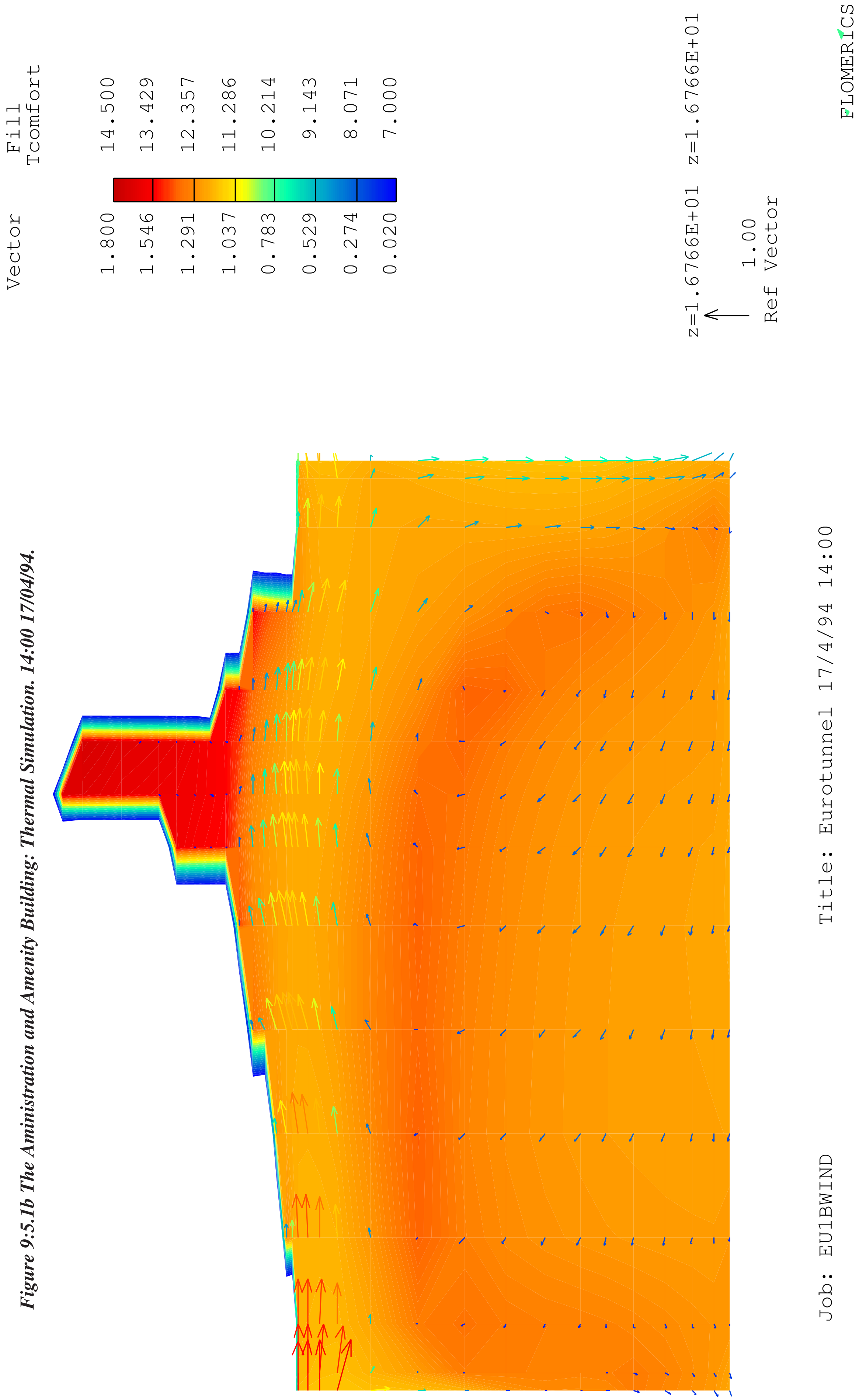

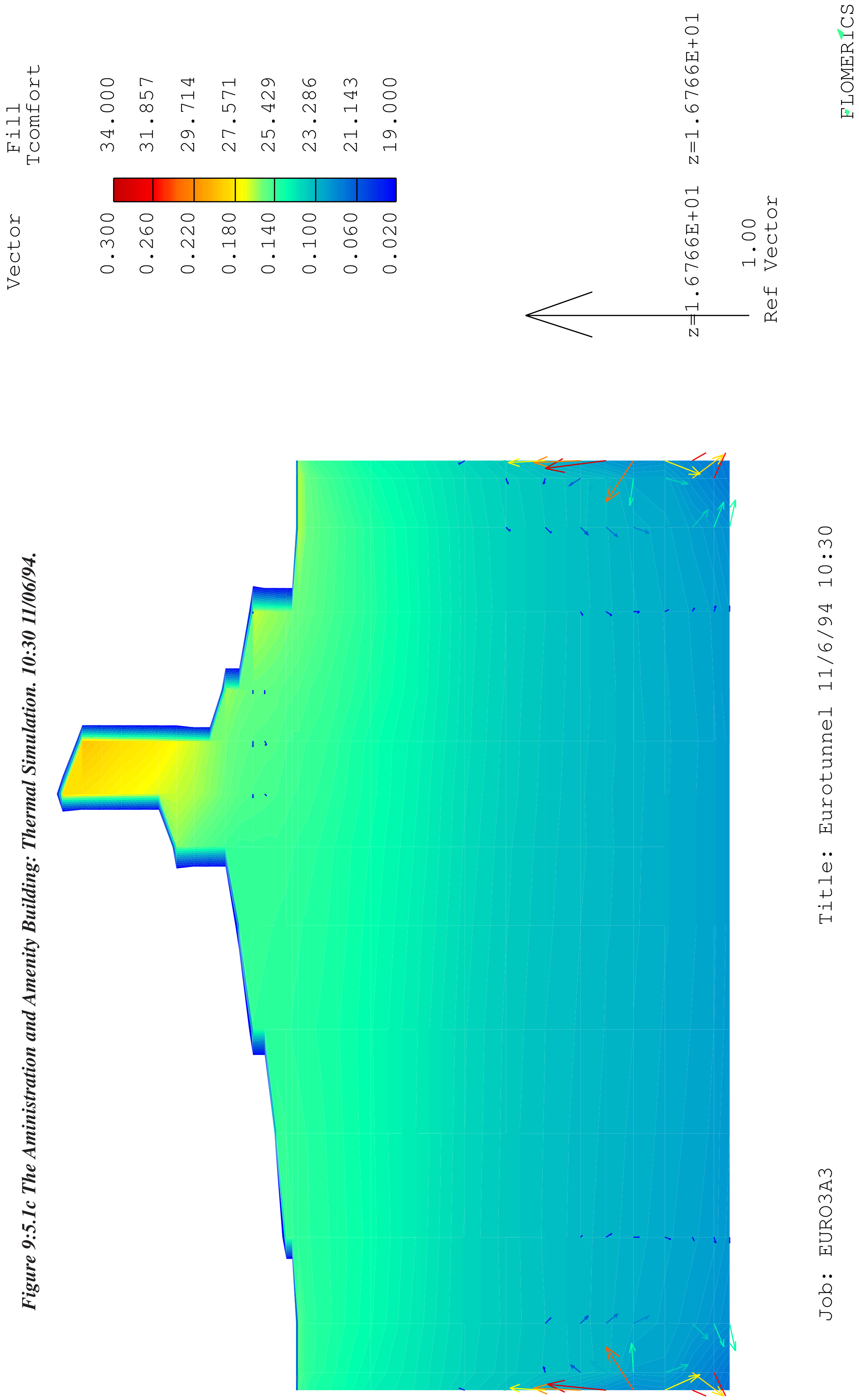

Figure 9:5.1c The Aministration and Amenity Building: Thermal Simulation. 10:30 11/06/94.

9:5.2 Comparison Between the CFD Model Output and the Data Monitored at the Administration and Amenity Building.

The relationship between the simulated behaviour shown in *Figures 9:5.1b* and *9:5.1c*, and the monitored data presented in Chapter 8 is illustrated below. The markers represent the relationship between the resultant temperatures monitored by the eleven sensors within the building and the temperatures predicted at those locations by *Flovent*, and the diagonal line represents the ideal relationship.

Figure 9:5.2 Graph to Illustrate the Relationship Between the Monitored and Predicted Resultant Temperatures Within the Administration and Amenity Building.

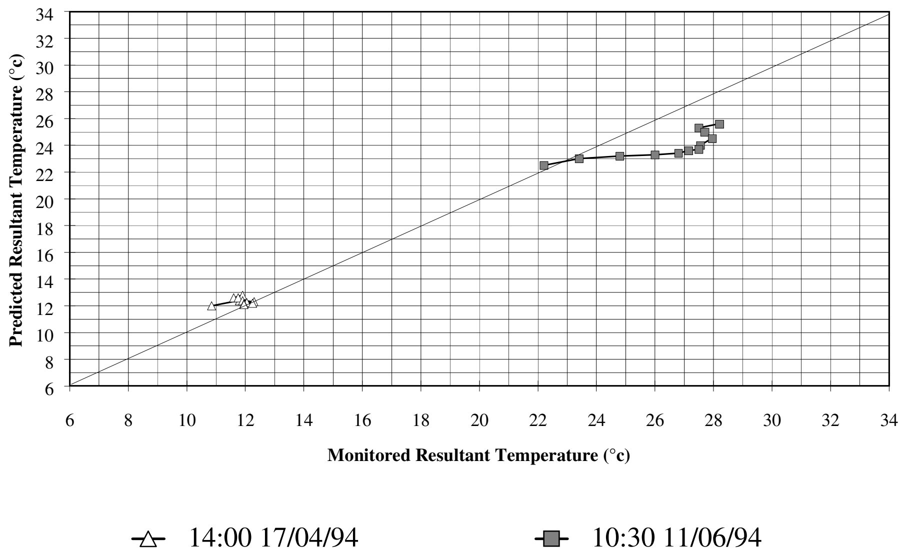

It proved impossible to accurately predict the monitored behaviour for the first simulation attempted (14:00 17/04/94) under the conditions in which the space was supposed to have existed. With no significant infiltration and bright sunshine, the model predicted an average internal resultant temperature almost 5^{o}c higher than the monitored value. If it was accepted however that the high level louvres were open, then the combination of perimeter infiltration and increased membrane internal surface convection reduced the average internal temperature to within 0.5^{o}c of the monitored value (as shown by *Figures 9:5.1b* and *9:5.2*). Based on the general accuracy of this simulation, it had to be concluded that the perimeter louvres had been open during this period, despite assurances from the Site Maintenance Manager that they had been closed.

The second simulation (*Figure 9:5.1c* 10:30 11/06/94) underestimated internal resultant temperatures by an average of almost 2.5^{o}c. Generally predictions close to the floor were accurate, but as the membrane was approached so internal resultant temperatures were increasingly underestimated. This meant that whilst stratification of 6^{o}c had been monitored within the space, stratification of just 3^{o}c was predicted.

Analysis of the monitored data presented in Chapter 8 had suggested that thermal gradients within this space resulted primarily from low level infiltration, suggesting that internal air temperatures were the main source of stratification. However whilst *Flovent* predicted internal radiant stratification of over 4^{o}c, the predicted stratification of air temperatures between the monitor points was just 2^{o}c. As with the previous spaces investigated therefore, it appeared that there was a problem within the fluid flow model.

Similar to the difficulties encountered with the Eisteddfod Arena Simulation, it seemed likely that this problem resulted from either an *underestimation of internal surface heat transfers*, of an *over diffusion of internal conditions*, as discussed below:-

- The complex form of the Administration and Amenity Building meant that it was necessary to represent its geometry in three dimensions. Even with a very course grid this required the specification of over 230 individual window panels in order to represent the shape of the fabric membrane. As a result of this the continuos double curvature of the membrane envelope was actually represented by a series of discrete steps. It was possible that this left the model unable to simulate the smooth flow of air along the underside of the membrane envelope. This could have resulted in the underestimation of surface convection heat transfers, and so the under prediction of internal stratification.

- The over diffusion of internal conditions could have resulted from the fact that *Flovent* was being used in its steady state mode, in order to simulate unsteady state situations. In order to achieve a stable solution, it was possible that internal air was being allowed to diffuse to an extent that would not have been possible under the continually changing conditions found in reality.

Both of these issues will be discussed further throughout the rest of this chapter.

9:6. MODELLING THE THERMAL BEHAVIOUR OF THE AELTC COVERED COURTS.

9:6.1 Specification of the AELTC Covered Courts.

It had generally been hoped that this space would be the easiest to simulate out of all of the buildings studied because of its simple, repetitive form. Initially therefore, the enclosure was specified as a two dimensional section, with low level *free openings* on the south east side and a single high level *extract fan* representative of the average rate of ventilation produced by the apex fans along the length of the building.

It was found however that this average value did not properly account for the variability of air movement within the space, resulting in air velocities being evened out along the length of the building, and so across the section being simulated. There was some likelihood that this would result in incorrect surface convection heat transfer calculations, and for this reason the space was re-specified as a three dimensional enclosure with point extract fans.

In an attempt to avoid some of the problems encountered in previous simulations, the slight double curvature of the envelope, and the slope of the end walls were ignored. This allowed a fine grid to be specified without unnecessarily increasing the complexity of this simulation. This produced a domain 47 cells long, 48 wide and 38 high, giving a total of over 63,000 cells. As with the other spaces simulated, the membrane was specified as a series of *window panels*, and the other surfaces forming the enclosure were specified as *boundary walls.*

Figure 9:6.1a The AELTC Covered Courts: Model Representation.

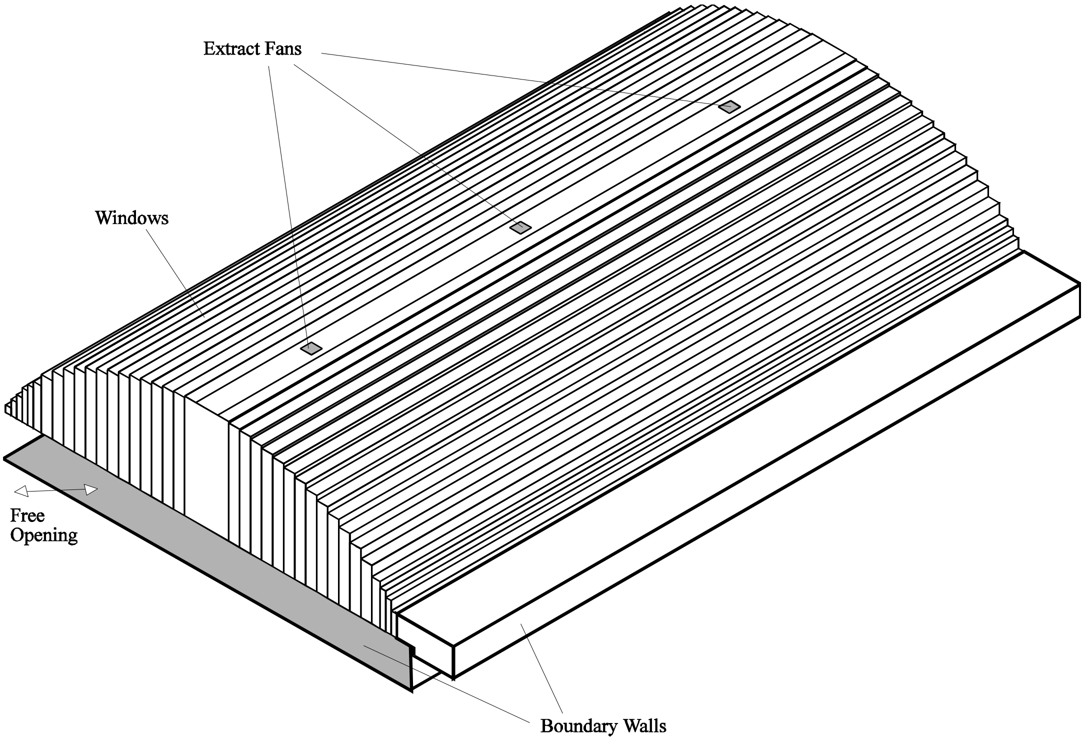

Figure 9:6.1b and 9:6.1c overleaf illustrate the internal resultant temperatures and internal air velocities predicted by two simulations based on the monitored data previously presented in Chapter 8. The first was based on data recorded when conditions within the space had been almost entirely diffuse (06:30 24/03/94), and the second based on data recorded when extreme positive stratification had been monitored within the space (12:00 27/07/95). It was considered reasonable to specify '*overhead*' solar radiation for both simulations as the transmittance of the membrane was relatively low, and there were few shading structures within the space.

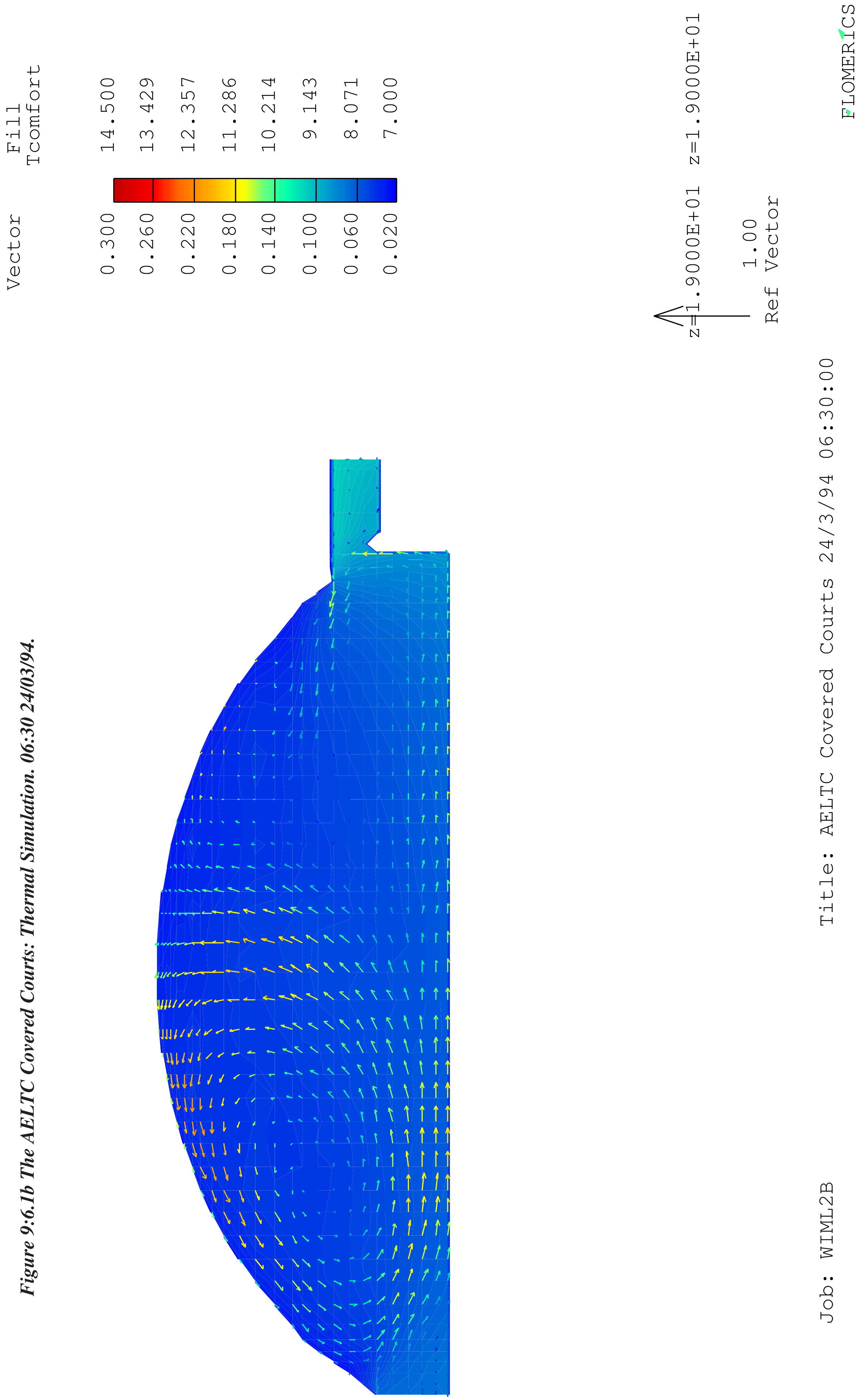

Figure 9:6.1b The AELTC Covered Courts: Thermal Simulation. 06:30 24/03/94.

Figure 9:6.1c The AELTC Covered Courts: Thermal Simulation. 12:00 27/07/94.

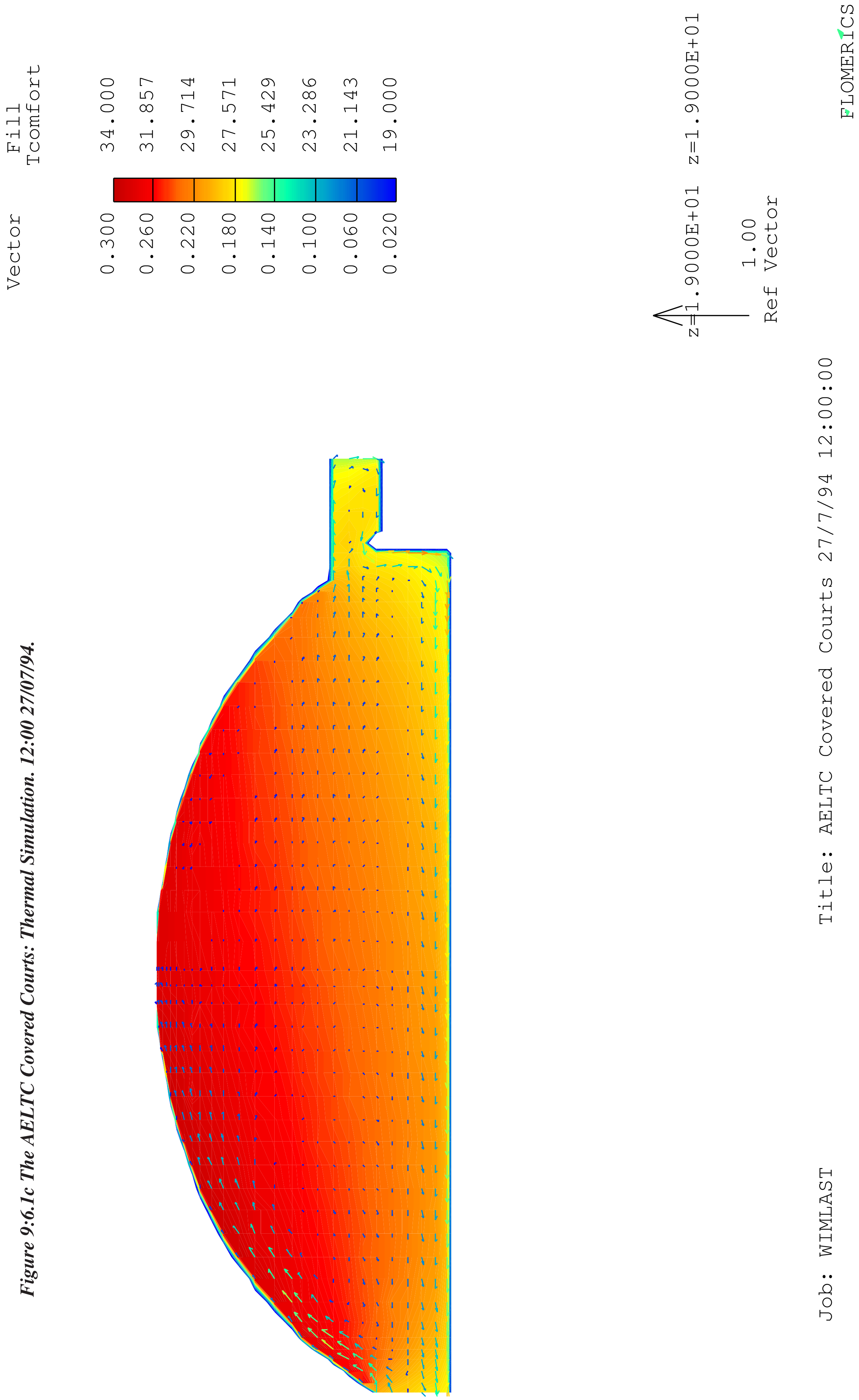

9:6.2 Comparison Between the CFD Model Output and the Data Monitored at the AELTC Covered Courts.

The relationship between the simulated behaviour shown in *Figures 9:6.1b* and *9:6.1c*, and the monitored data presented in Chapter 8 is illustrated below. The markers represent the actual relationship between the resultant temperatures monitored by the eleven sensors within the building, and the temperatures predicted at those locations by *Flovent*, and the diagonal line represents the ideal relationship.

Figure 9:6.2 Graph to Illustrate the Relationship Between the Monitored and Predicted Resultant Temperatures Within the AELTC Covered Courts.

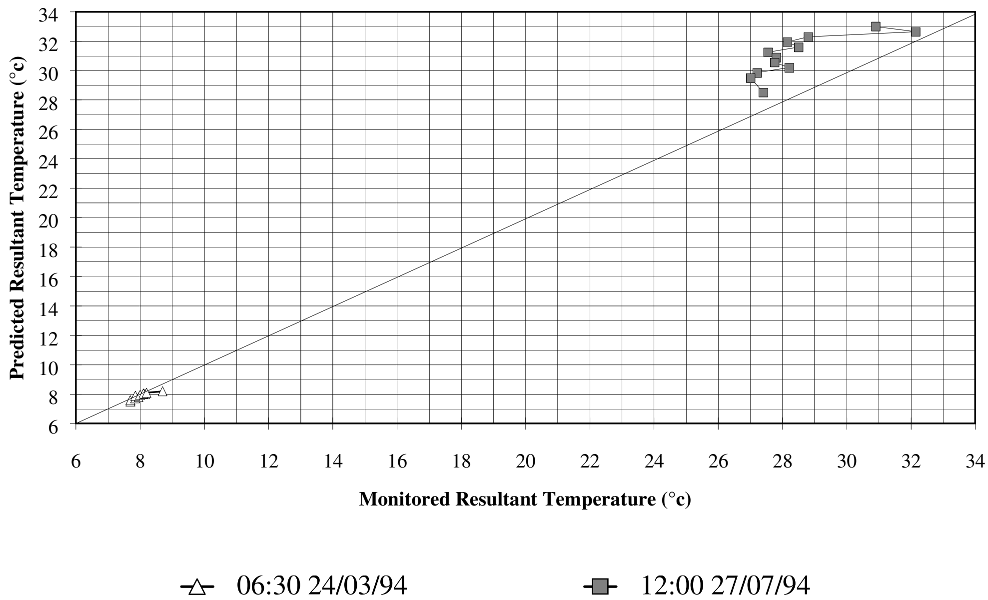

As with all of the spaces modelled, *Flovent* simulated the *diffuse* conditions within the AELTC Covered Courts (06:30 24/03/94 illustrated by *Figure 9:6.1b*) fairly accurately. It can be seen from *Figure 9:6.2a* that the resultant temperatures predicted by the first simulation were all within 0.5^{o}c of the monitored values, and the average model error was just 0.1^{o}c.

The average difference between the monitored resultant temperatures, and those predicted by the second simulation (12:00 27/07/94 illustrated by *Figure 9:6.1c*) was 2.6^{o}c. It can be seen from *Figure 9:6.2* however that *Flovent* predicted the extent of stratification within the space fairly accurately, and as a consequence the maximum difference between the predicted and monitored values was just 3.8^{o}c. An internal resultant temperature gradient of 4.5^{o}c was predicted, just 0.7^{o}c less than the monitored value, and this included internal air stratification of over 4^{o}c. This suggested that the problems encountered whilst simulating the previous spaces described in this chapter, were not as significant in the case of the AELTC Covered Courts.

It was considered that this improved accuracy resulted form a number of the design features of the space itself:-

- The membrane enclosing the space was tinted green on its outer surface and this gave it a particularly high solar absorptance, suggesting that it was likely to be more diffusing than the other membranes investigated. This combined with the lack of any significant shading structures within the enclosure meant that all the internal temperature sensors were likely to have been exposed to a similar intensity of solar radiation.

- The simple, repetitive section of the AELTC Covered Courts was easier to specify in three dimensions than the previous spaces. As a consequence of this it was possible to refine the grid spacing applied to the domain without greatly increasing the computational time necessary to carry out simulations.

- Three extract fans were constantly forcing air through the space, producing relatively high internal air velocities along the underside of the membrane. This resulted in increased surface convection heat transfers being predicted, and also meant that internal air was less likely to diffuse down into the lower levels of the space as a result of *Flovent* converging on a steady state solution.

The improved ability to predict internal stratification within this space compared to the three previous case studies is characteristic of the performance of CFD models in general.

Simple spaces tend to be the easiest to model, and in particular, solutions are more realistic in cases where strong ventilation generates obvious internal air movement patterns. Complex, naturally ventilated spaces however require very precise specification as their fluid behaviour results entirely from surface heat transfers. In the case of spaces enclosed by fabric membranes, this level of specification can be practicably impossible to provide, and so fluid flow predictions can prove inaccurate.

These issues will be discussed further in the next section of this chapter, and again in Chapter 10.

9:7 SUMMARY OF THE FINDINGS OF THE MODELLING PROCESS.

9:7.1 The Overall Accuracy of the CFD Simulations.

In this section, the overall accuracy of the *Flovent* simulations is summarised, and the reasons for some of the difficulties encountered are discussed.

The graph below illustrates the overall relationship between the monitored data presented in Chapter 8 and the internal resultant temperatures predicted by the eight simulations described in this chapter. The diagonal line represents the '*ideal*' relationship, indicative of where the markers would be if there were no difference between the monitored and predicted values.

Figure 9:7.1a Graph to Illustrate the Relationship Between the CFD Simulations and the Monitored Data.

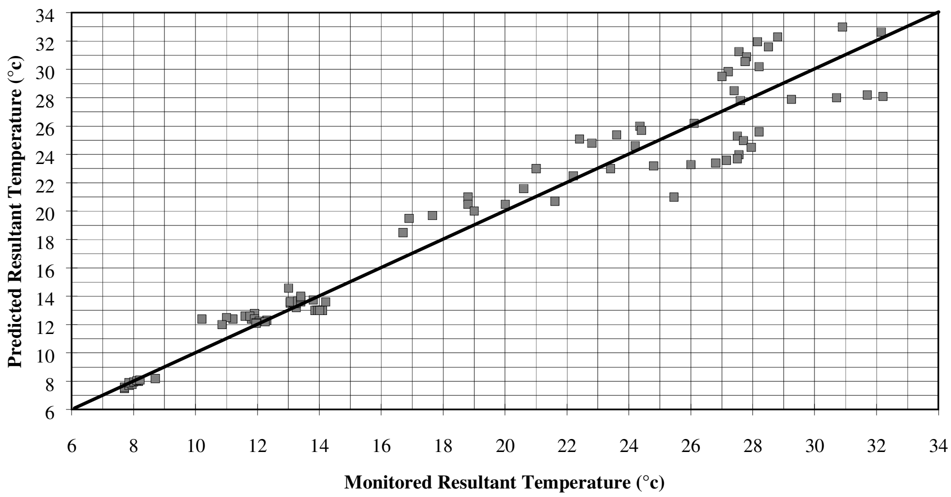

It can be seen that generally the predicted values followed the monitored behaviour closely. The average difference between the monitored and predicted values was less than 1.5^{o}c, and the maximum error was just 4.5^{o}c. Irrespective of the problems encountered, it was considered that this must be a significant improvement on the techniques used by previous researchers, who had based much of their boundary analysis on the use of U-values and shading coefficients and who for the most part had completely ignored the affects of internal stratification.

It was apparent however that as the temperature within the spaces increased, so did the spread of predicted values about the ideal. This appeared to result from the fact that strong internal stratification could be generated during hotter conditions, and the extent of this stratification was generally under predicted by *Flovent*. This is clearly shown by the graph below.

Figure 9:7.1b Diagram to Show the Relationship Between the Extent of Monitored Internal Stratification and the Accuracy of the Internal Resultant Temperatures Predicted by Flovent.

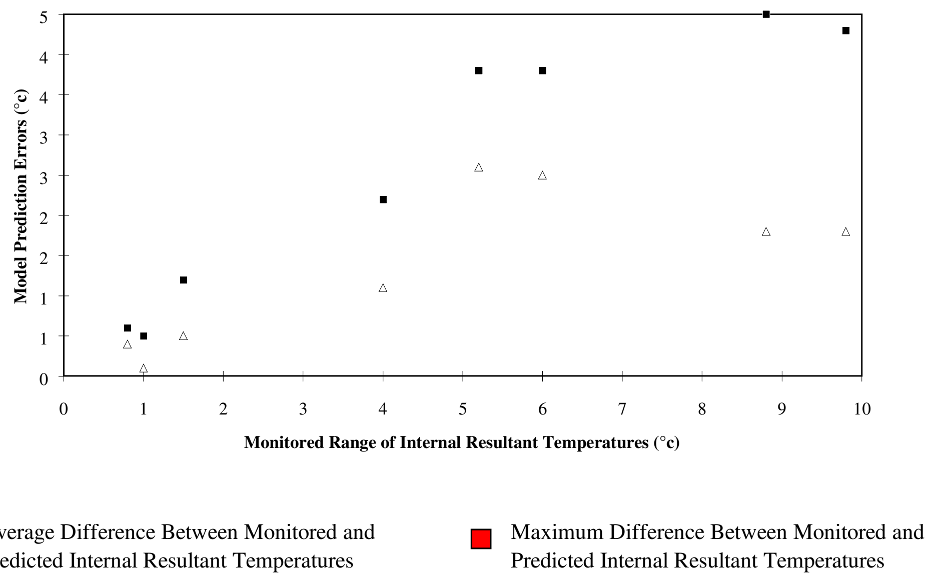

It was not considered that the tendency for *Flovent* to under predict stratification within the spaces simulated could be explained by inaccuracies within the monitored data. External conditions were monitored using standard meteorological apparatus, and the calibration of the exposed thermistors used to monitor internal conditions (*Figure 8:2.2*) suggested that if anything they would underestimate the extent of thermal stratification.

In order to validate the use of exposed thermistors in actual buildings however, a position had been chosen close to the membrane within each of the spaces investigated at which to monitor both globe, and exposed thermistor temperatures. The maximum difference between recorded globe and thermistor values within the spaces studied was 2.5^{o}c, but on average the difference was just 0.4^{o}c. There was a general tendency for the exposed thermistors to underestimate globe temperatures, and this suggested the *Flovent* should have predicted stronger thermal gradients than had been monitored. *Flovent* actually underestimated the stratification of resultant temperatures and this suggested that there was a problem within the modelling process itself.

Resultant temperatures were predicted by *Flovent* based on the standard CIBSE equation based on *radiant temperatures* (including *solar radiation*), *air velocities and air temperatures* each of which is discussed in turn below.

- The process used by Flovent to predict *radiant temperatures* is well established based on the geometric relationship between the surfaces of specified temperature which enclosed the space. If the geometry and temperatures of internal surface are accurately specified, there is no reason why any significant error should be incurred in these calculations. Indeed, the validation of the boundary model presented in Chapter 7 suggested that if anything, the temperature of the membrane was likely to be overestimated which should have resulted in internal radiant stratification being over predicted.

- Because of the complex optical properties of fabric membranes and the simplicity of the solar model within *Flovent,* there were problems specifying the distribution of solar radiation within the spaces simulated. It was considered however that at worst this would cause the stratification of internal resultant temperatures to be underestimated by 2.5^{o}c, and under most circumstances the actual error would be considerably less than this.

- *Air velocities* were exceptionally sensitive to the problem specification. Whilst realistic internal air movement patterns could be predicted fairly confidently in spaces with strong, active ventilation systems, this tended not to be the case in more complex naturally ventilated or sealed spaces. When internal air movement patterns were not '*obvious*', it was found that slight variations in the way that simulations were set up could completely change the model predictions.

- As a consequence of this, internal *air temperatures* were also sensitive to the way that the problem was specified, tending to under predict the stratification of the internal air.

The overall result of this was that *internal resultant temperatures,* which were a product of all of these variables were not inaccurate, although the extent of internal stratification tended to be under predicted. This is shown clearly by the graph below.

Figure 9:7.1c Diagram to Show the Relationship Between the Monitored stratification of Internal Resultant Temperatures, and the Various Thermal Gradients Predicted by Flovent.

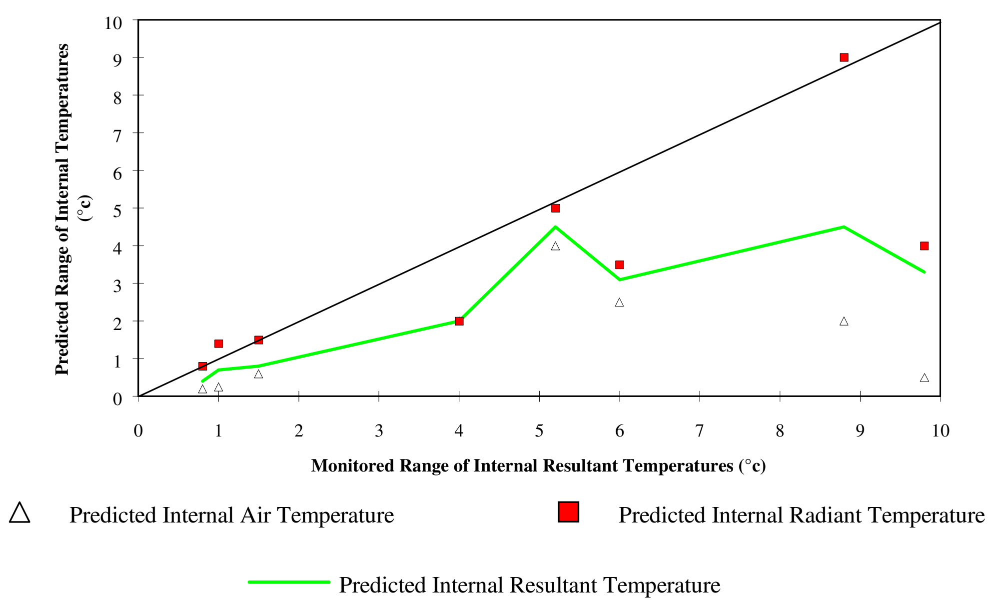

It was considered therefore that the tendency for *Flovent* to under predict internal stratification resulted predominately from problems within the fluid flow model itself, and some of the possible reasons for this will now be discussed.

9:7.2 Analysis of the Fluid Flow Model.

The fluid flow problem specification was previously defined as consisting of two basic categories:-

- *boundary conditions*.
- *fluid properties*.

Within these categories however it was actually only appropriate for the model user themselves to specify four variables:-

- The turbulent viscosity of the enclosed air.
- The quantity of air allowed into or out of the enclosure by its boundaries.
- The surface temperatures of the enclosure boundaries
- The geometry of the enclosure boundaries.

The likelihood of any of these four variables causing *Flovent* to underestimate the extent of thermal stratification within the spaces simulated is discussed below.

- *Turbulent viscosity* was calculated within each individual cell for all of the simulations using the complex Ke model of turbulence, and so this in itself was unlikely to be the source of a major problem.

- The quantity of *air* allowed into or out of the enclosure by its boundaries was determined either from the monitored data or from manufacturers information describing mechanical ventilation systems. As some of the simulations carried out had involved completely unventilated spaces, it seemed unlikely that this was the source of a consistent problem.

- The *surface temperatures* within the space were either taken from monitored data, or they were predicted using the boundary model described in chapter 7. The CFD predictions were relatively insensitive to the small range within which these values could realistically be varied, and it had been shown that if anything, the boundary model was likely to overestimate membrane internal surface temperatures. This would be expected to result in stratification being over predicted not under predicted.

Unfortunately however, *Flovent* did not have any facility for varying surface temperatures from one time step to the next, and this meant that *transient* simulations could not be attempted. There was some possibility that the process of converging on *steady state* solutions resulted in internal air temperatures being allowed to diffused to an extent which in reality the changeability of conditions would have made impossible.

There was little monitored data however to suggest that stratification did diffuse significantly through time within such spaces. Even when conditions remained constant for long periods of time, hot, high level air only slowly spread to lower levels and as this seldom reached the floor, it tended not to affect the overall all extent of stratification.

In order to investigate this problem further, a series of simple transient simulations were attempted using both *Flovent* and *DFS Air*[13], a CFD package which allowed surface temperatures be changed over time. These provided no evidence to suggest that long term diffusion would significantly affect the overall range of temperatures within such spaces. Results however were generally inconclusive, and so it was still considered that this could be a contributing factor to the overall underestimation of stratification.

- It was likely however that much of the uncertainty associated with the fluid flow model resulted from the specification of the enclosure *geometry*. In particular, there were doubts regarding the membrane internal surface convection heat transfers because of the stepped geometry which had to be used to represent their double curvature.

Fabric membranes can be significantly hotter or colder than the air within the spaces they enclose, particularly during periods of strong stratification, and it is possible that this generates fast moving air streams close to the underside of their continuous smoothly curving surface. If *Flovent* was unable to properly simulate these air streams, it would have significantly underestimated internal surface convection heat transfers resulting in an underestimation of internal stratification.

This is similar to the situation found close to cold windows, were strong down draughts can result in a significant increase in internal surface convection heat transfers. Flomerics recommend that in order to properly simulate this phenomena, it is necessary to increase the detail with which the air flow close to such surfaces is simulated, and this can be done by refining the boundary layer grid size to around 100mm[14].

Because of the stepped representation of the fabric membranes however, such a decrease in grid spacing greatly increases the complexity of the problem specification and the computational time required to converge upon a solution. The reason for this is illustrated schematically by the series of diagrams overleaf.

Figure 9:7.2a Diagram to Illustrate the Grid Refinement Necessary in Order to Allow Fast Moving Air Streams at Cold Window Surfaces to be Predicted.

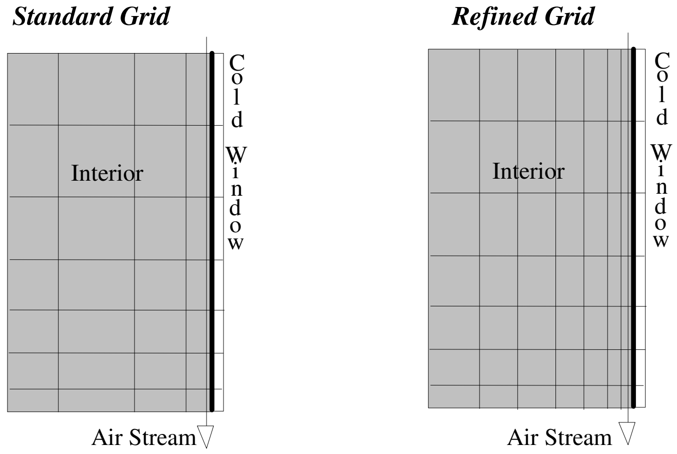

Figure 9:7.2b Diagram to Illustrate the Grid and Surface Refinement Necessary in Order to Allow Fast Moving Air Streams at Curved Surfaces to be Predicted.

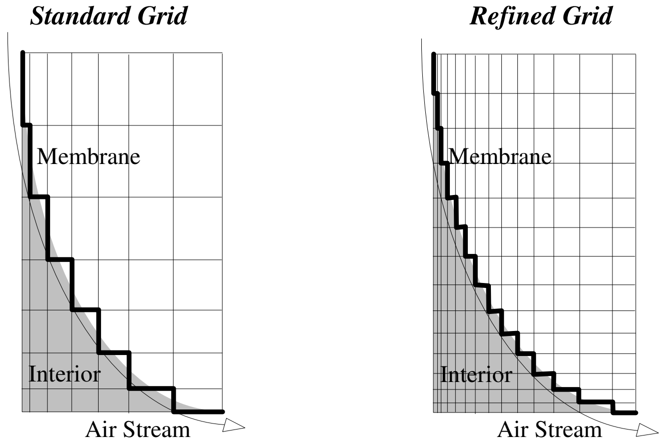

It can be seen that for conventional horizontal or vertical surfaces, boundary layer refinement is relatively simple to apply, merely requiring that additional grid lines are placed perpendicular to the surface being investigated. In the case of curved surfaces however gird refinement must take place in both the horizontal and vertical planes and this incurs a large computational overhead. Such refinement also requires that the geometry of the surface itself is refined and this increases the complexity of the boundary specification. In three dimensional simulations, the situation is complicated further and both the surface specification and computational overhead become impracticable.

The extent of this problem is difficult to quantify as surface air velocities are highly dependant upon the exact details of the situation being simulated. It was however anticipated that it would most significantly affect the accuracy of predicted fluid flow patterns when there was a strong contrast between the temperature of the membrane and that of the enclosed air, i.e. during periods of stratification. This would result in the extent of stratification being under estimated.

In the next chapter, an alternate method of refining the boundary specification in order to overcome this problem is discussed.

9:8. CONCLUSION.

In this chapter the approach necessary in order to simulate the thermal behaviour of spaces enclosed by fabric membrane envelopes was discussed. It was considered that Computational Fluid Dynamic techniques were required, and to that end *Flovent,* a commercial CFD model was selected. A series of simulations carried out using *Flovent* were then described and the accuracy of those simulations was tested against the monitored data presented in Chapter 8.

It was found that the average difference between the resultant temperatures predicted by *Flovent* and those monitored within the buildings simulated was just 1.4^{o}c, and all the predicted values were within 4.5^{o}c of the monitored data. It was considered that this must be a significant improvement on the work of previous researchers, who had tended to base their boundary analysis on U-values and shading coefficients and who had largely ignored internal stratification.

Generally, simple spaces tended to be the easiest to simulate, and in particular solutions were more realistic when strong internal ventilation generated obvious air movement patterns. The simulations did however show a tendency to under predict the extent of the internal thermal stratification particularly during '*hot*' conditions. There was some possibility that this resulted from the oversimplified nature of the solar model, and the adoption of a *steady state* rather than a *transient* approach to the simulations, however it seemed likely that the problem was caused primarily by the geometrical representation of the spaces simulated.

The model specification was based entirely upon the adoption of a Cartesian grid, and as a result, doubly curved membrane surfaces had to be represented as a series of '*stepped*' horizontal and vertical panels. Specifying curves in this way meant that it was practicably impossible to refine the detail with which air flow close to membrane surfaces was simulated. It was likely that this left the model unable to predict fast moving air streams close to the membranes, and as a result internal surface convection heat transfers were under predicted.

In the next chapter, an approach which may be adopted in order to avoid these problems will be described along with a general discussion of the research presented in the rest of this thesis.

---

1 CIBSE; *CIBSE Guide: Volume A, Design Data,* The Chartered Institute of Building Service Engineers, London, 1986, PA1-4.

2 Collins Dictionaries, *Collins English Dictionary*, Harpers Collins Publishers, Glasgow, Third Edition, 1991, P593.

3 Rubini, P; Engelbrcht, G; "Computational Fluid Dynamics." *Computational Fluid Dynamics and Combustion Modelling Group*, Cranfield University, November 1994.

4 Harries, N; *Computational Modelling of the Internal Environment of Industrial Buildings with Overhead Radiant Heating Systems*, PhD, University of Wales College of Cardiff, 1994, P12.

5 Tomasz, P; "CFD Codes List", *Netscape,* http://www.mpa-garching.mpg.de/~tomek/CFD/CFD_codes.html, 19/12/95.

6 Liddament, M. W; *A Review of Building Air Flow Simulation*, Annex V Air Infiltration Centre, Coventry, March 1991, P9.

7 ibid. Liddament, M. W; *A Review of ...,* Appendix 3.

8 Flomerics; *Flovent Reference Manual*, Flomerics Ltd, Surrey, Version 1.4, 1994, Pxx.

9 ibid. Flomerics; *Flovent Reference Manual*, Pxiv.

10 ibid. Flomerics; *Flovent Reference Manual*, P3:4.

11 ibid. Flomerics; *Flovent Reference Manual*, P2:12.

12 ibid. Flomerics; *Flovent Reference Manual*, PGLO-6.

13 *DFS Air*, Design Flow Solutions, Mark 4, Revision B, 1994.

14 ibid. Flomerics; *Flovent Reference Manual*, Version 1.4, Pxii.